Remec, I.[1]

Impact of the ENDF/B-VI Cross Sections on the RPV Fluence Determination

---

Reference: Remec, I., **"Impact of the ENDF/B-VI Cross Sections on the RPV Fluence Determination,"** Reactor Dosimetry, ASTM STP 1398, John G. Williams, David W. Vehar, Frank H. Ruddy and David M. Gilliam, Eds., American Society for Testing and Materials, West Conshohoken, PA, 2000.

Abstract: The calculations with the broad-group cross-section library Bugle-96, and atom displacement (dpa) cross sections for iron, both derived from ENDF/B-VI data, result in higher calculated fast neutron fluxes, better agreement of calculations with radiometric dosimeter measurements, and significantly slower dpa rate attenuation through pressure vessel walls relative to the results with their predecessors: the Sailor library and ASTM iron dpa cross sections.

Keywords: ENDF/B-VI, neutron transport, dosimetry, reactor pressure vessel

---

INTRODUCTION

The accuracy and reliability of the pressure vessel (PV) flux calculations depend critically on the neutron cross sections. A continuous quest for improvements led, in the early 1980s, to the development of the Bugle-80 and Sailor broad-group libraries from the ENDF/B-IV data and, in 1996, to the Bugle-96 library from the ENDF/B-VI data [*1-3*]. Bugle-80 and Sailor were recommended and used extensively for deterministic PV flux calculations for almost two decades, and a large body of results is available for inter-comparisons. However, only a few results with the currently recommended Bugle-96 have been published to date [*4*]. The first part of this paper investigates the impact of the change from the Sailor to the Bugle-96 library on the results of transport calculations, namely, the calculated PV fast flux, the energy spectrum, and the comparison of calculated dosimeter responses with measurements. In the second part, the new atom displacement (dpa) cross sections for iron, which were developed from the ENDF/B-VI data are discussed and compared to the dpa cross sections from the ASTM standard [*5*]. The final part of the paper discusses the effects of the changes of the cross-section library and dpa cross sections on the flux and dpa attenuation in the PV wall. This work was sponsored by the Office of Nuclear Regulatory Research, U. S. Nuclear Regulatory Commission, as part of the "Embrittlement Data Base and Dosimetry Evaluation Program."

---

[1]Oak Ridge National Laboratory, MS 6363, P.O. Box 2008, Oak Ridge, TN 37831-6363, USA.

TRANSPORT CALCULATIONS

The study was performed for the H. B. Robinson-2 (HBR-2) power plant, which is a 2300-MW (thermal) pressurized light-water reactor designed by Westinghouse. All plant data, including the power distribution and the dosimetry measurements, were taken from the HBR-2 benchmark [*6*]. The transport calculations were performed using the DORT computer code and a flux synthesis method [*7*]. The flux synthesis method uses one- and two-dimensional transport calculations to obtain the neutron flux in three-dimensional geometries. All calculations were performed as fixed neutron source calculations with a P_3 expansion of the angular dependence of the scattering cross sections, and a symmetric S_8 "directional quadrature set." The same calculational procedure, models, and code numerical parameters were used for all the calculations [*6,8*]. The only data varied were the cross sections for the transport and the fission spectrum of the neutron source.

The Sailor and Bugle-96 libraries have the same neutron energy group structure with 47 groups. Detailed comparisons of the calculated multigroup spectra in the surveillance capsule (attached to the thermal shield in the downcomer), and in the reactor cavity (at the location of dosimeters), are presented in Fig. 1. Over most of the energy range, Bugle-96 gives higher group fluxes. For most of the energy groups above 0.1 MeV, the increases are in the range ~5–10% in the capsule and 20–40% in the cavity. This pattern changes above ~5MeV, where Sailor predicts up to two times higher group fluxes than Bugle-96, both in the capsule and in the cavity. The only other difference between the calculations compared in Fig. 1, besides the cross-section libraries, was the spectrum of the fission neutrons. In both calculations the fission spectrum was assumed to be the average of the ^{235}U and ^{239}Pu fission spectra. However, for the calculation with Bugle-96, the spectra were taken from the Bugle-96 library, and for Sailor calculation from the Sailor library. (The ^{239}Pu fission spectrum is not available in Sailor and was collapsed from the Vitamin–C library, which is the fine-group library from which Sailor was generated.) The fission spectra from the two libraries are compared in Fig. 2. Large differences at the scarcely populated high-energy end are obvious and are readily reflected in the change of the spectra shown in Fig. 1. Finally, the Sailor calculation was repeated with the fission spectra from Bugle-96. This calculation is compared to the Bugle-96 results in Fig. 3. The shapes of the curves in Fig. 3 and Fig. 1 at high-energy are significantly different, confirming that the decrease in Bugle-96-to-Sailor group-flux ratios in Fig. 1 is indeed caused by the differences in the fission spectra. The differences in Fig. 3 are due to the change of cross sections only, and are, below ~5MeV, somewhat larger than those in Fig. 1. Over most of the energy range of importance for PV embrittlement, the differences in the calculated spectra are dominated by the changes in the cross sections. The high-energy part; however, is substantially affected by the differences in the fission spectra.

The calculated fast fluxes ($\phi_{E>1MeV}$) are compared in Table 1. Bugle-96 calculations give ~6% higher fast fluxes in the capsule and at the PV inner surface, ~10% higher $\phi_{E>1MeV}$ at 1/4 of the PV wall, and ~25% higher $\phi_{E>1MeV}$ in the cavity. The differences in the fission spectra cause only 3-4% changes in the fast flux, with Bugle-96 fission spectra resulting in lower $\phi_{E>1MeV}$ values.

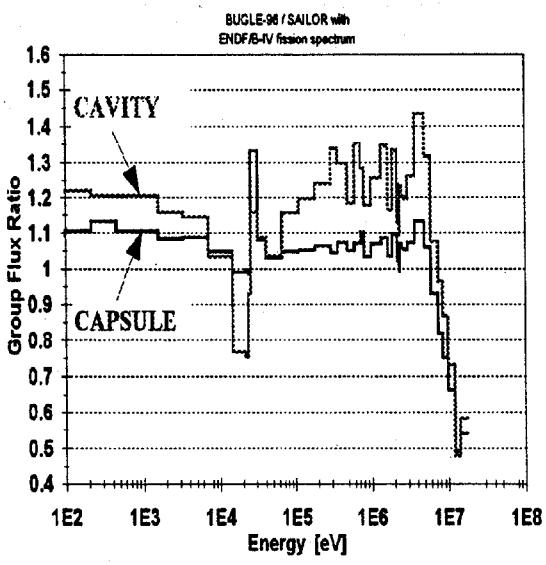

Figure 1. The ratios of the group fluxes (Bugle-96/Sailor) library in the surveillance capsule and at the location of dosimeters in the cavity. The calculations with the Sailor library utilized Sailor fission spectra

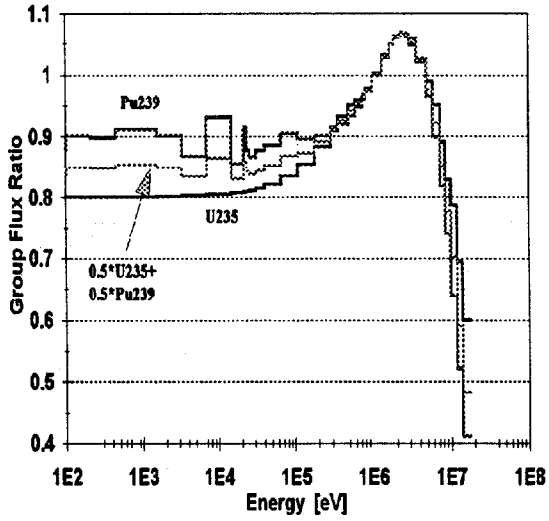

Figure 2. The ratios of fission spectra (Bugle-96/Sailor) for the ^{235}U, ^{239}Pu, and the average of the ^{235}U and ^{239}Pu spectra, from the Bugle-96 and Sailor libraries

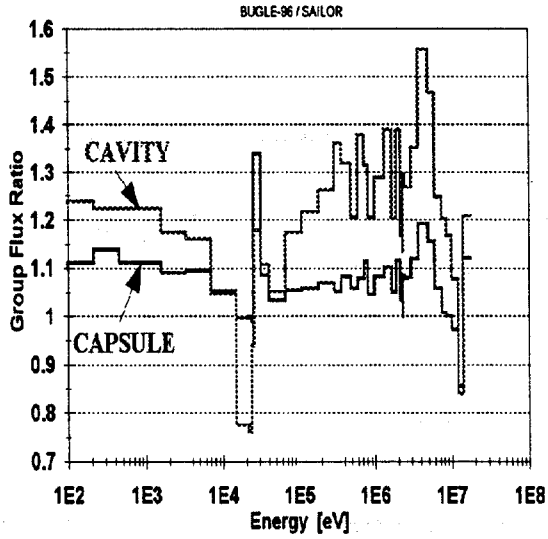

Figure 3. The ratios of the group fluxes, calculated with the Bugle-96 and Sailor libraries, in the surveillance capsule and in the cavity. Bugle-96 fission spectra were used for both transport calculations

The calculated reaction rates are compared with the measurements in Table 2. The Bugle-96 and "Sailor with Sailor fission spectrum" gave about the same average C/M ratio in the capsule, while in the cavity the Bugle-96 value is ~10% higher. The differences in the average C/M values between the Bugle-96 and the "Sailor with Bugle-96 fission spectrum" are much larger and are ~8% in the capsule and 28% in the cavity. The changes in the fission spectra from the Sailor to the Bugle-96 library are obviously very important for the comparison of the calculations with the measurements. This observation is reinforced by the comparison of two Sailor calculations— one with the Bugle-96 fission spectra and one with the Sailor fission spectra. The calculation with the Sailor fission spectra gave a 12% higher C/M value in the capsule and a 17% higher value in the cavity. The calculations with Bugle-96 fission spectra, both with Bugle-96 and Sailor cross sections, show a relatively small spread of the C/M values for the dosimeters with different reaction thresholds and

consequently small standard deviations of the average C/Ms, which are only 4-5% in the capsule and 7-8% in the cavity. For the calculation with the Sailor fission spectra, the corresponding standard deviations are 11% in the capsule and 17% in the cavity. Furthermore, the C/M ratios in the calculation with the Sailor fission spectra increase systematically from the lower- to higher-threshold dosimeters, especially in the cavity, with particularly high C/M values for the highest threshold dosimeter (^{63}Cu). This trend is much smaller in the Sailor calculation with the Bugle-96 fission spectra and is not present in the Bugle-96 results. These observations indicate that the change from the Sailor to the Bugle-96 fission spectra improves the agreement of the calculated spectra with the actual spectra during the irradiation.

Table 1. Comparison of the fast fluxes (E > 1 MeV) calculated with Sailor and Bugle-96 libraries

	$\phi_{E>1MeV}$ ($cm^{-2}s^{-1}$)			Ratio	
	Sailor + Sailor Fiss. Spec.	Sailor + Bugle-96 Fiss. Spec	Bugle-96	(Sailor + Bugle-96 Fiss. Spec.)/ (Sailor + Sailor Fiss. Spec.)	Bugle-96/ (Sailor + Sailor Fiss. Spec.)
Capsule	3.943E+10	3.852E+10	4.175E+10	0.97	1.06
PV inner radius	2.872E+10	2.792E+10	3.042E+10	0.97	1.06
1/4 T PV	1.468E+10	1.425E+10	1.611E+10	0.97	1.10
Cavity	6.214E+8	5.969E+8	7.793E+8	0.96	1.25

Table 2. The C/M ratios for the Bugle-96 and Sailor libraries

	^{237}Np (n,f) ^{137}Cs	^{238}U (n,f) ^{137}Cs	^{58}Ni (n,p) ^{58}Co	^{54}Fe (n,p) ^{54}Mn	^{46}Ti (n,p) ^{46}Sc	^{63}Cu (n,α) ^{60}Co	Ave. C/M $\pm \sigma$
Capsule							
Bugle-96	0.92	0.89	0.96	0.93	0.85	0.93	0.91 ± 0.04
Sailor + Bugle-96 fiss. spectra	0.85	0.82	0.86	0.84	0.78	0.90	0.84 ± 0.04
Sailor + Sailor fiss. spectra	0.88	0.86	0.94	0.92	0.93	1.13	0.94 ± 0.10
Cavity							
Bugle-96		0.82	0.97	0.96	0.90	0.96	0.92 ± 0.06
Sailor + Bugle-96 fiss. spectra		0.63	0.73	0.71	0.71	0.80	0.72 ± 0.06
Sailor + Sailor fiss. spectra		0.67	0.81	0.80	0.87	1.06	0.84 ± 0.14

ATOM DISPLACEMENT CROSS SECTIONS FOR IRON

In the current methodology for the determination of the radiation embrittlement of reactor vessel materials, as described in the U.S. Nuclear Regulatory Commission Regulatory Guide (RG) 1.99, Rev. 2, the calculated dpa is used as an alternative method for determining the fast-fluence attenuation in the PV wall [*9*]. The dpa cross sections given in the ASTM Standard Practice E 693 are based on ENDF/B-IV data. The new dpa cross sections were generated from the ENDF/B-VI (Release 3) data, using the same procedure and assumptions (to the extent possible) which were applied in the preparation of the "ASTM" dpa. Since ENDF/B-VI gives data for individual iron isotopes, they were processed separately and then combined. The contributions of the individual isotopes to the dpa cross sections for natural iron are shown in Fig. 4. Fig. 5 shows the differences between the new (ENDF/B-VI) and ASTM dpa cross sections. Detailed comparisons of the integral dpa rates obtained with the new and ASTM dpa cross sections were performed for the calculated neutron spectra throughout the HBR-2 PV thickness. The differences in dpa rates were relatively small and showed systematic variation from the PV inner wall, where new cross sections gave ~0.4% lower dpa rate, towards the outer wall, where the new dpa cross section gave ~4% higher dpa rate [*10*].

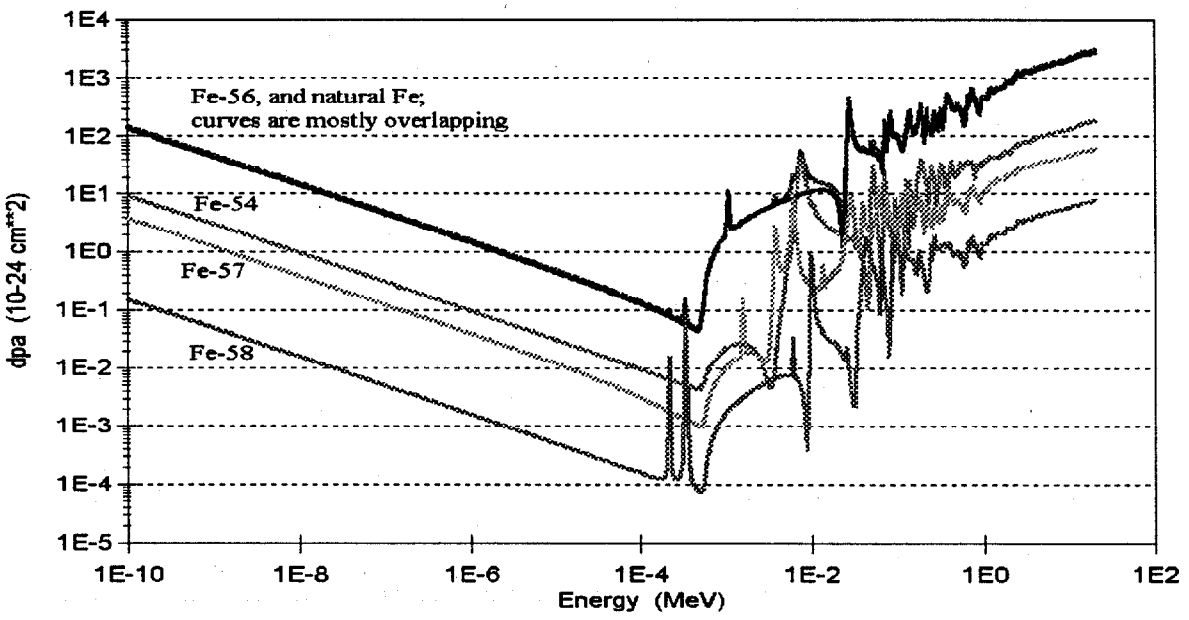

Figure 4. Contributions of individual isotopes to the displacement cross section for natural iron

FAST FLUX AND DPA ATTENUATION IN THE PV WALL

The fast flux and dpa attenuation through the PV wall, again for the HBR-2 reactor, as calculated with the Sailor and Bugle-96 cross-section libraries, and ASTM and new (ENDF/B-VI) dpa cross sections, is illustrated in Fig. 6. The curve representing the RG 1.99, Rev. 2 attenuation formula, which was derived from the calculations of several reactors with pre-ENDF/B-IV cross sections and a P_1 approximation, is also shown [*11*].

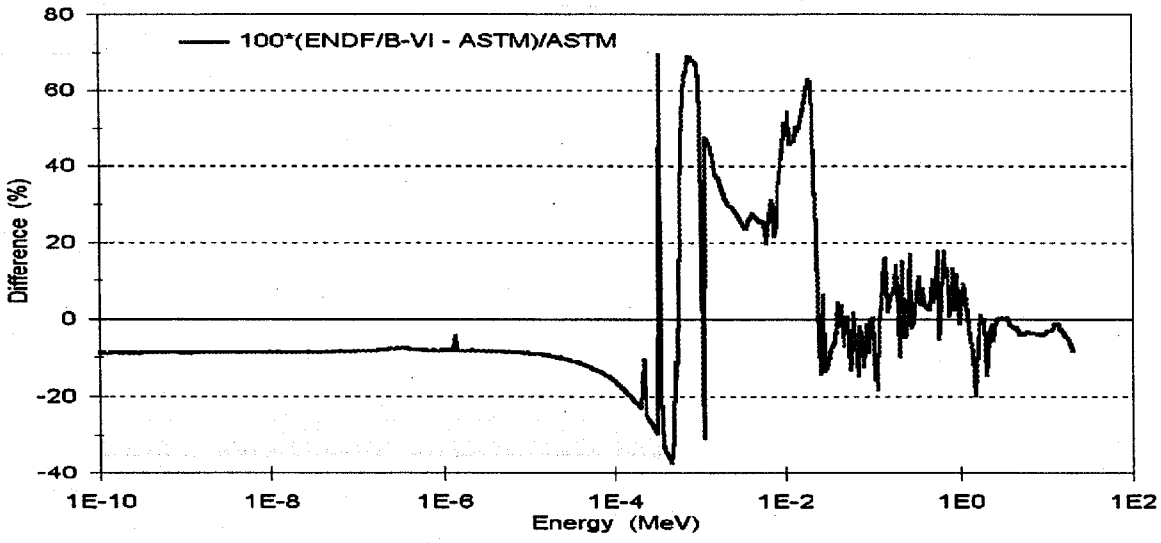

Figure 5. Differences in ENDF-B/VI and ASTM dpa cross sections for iron

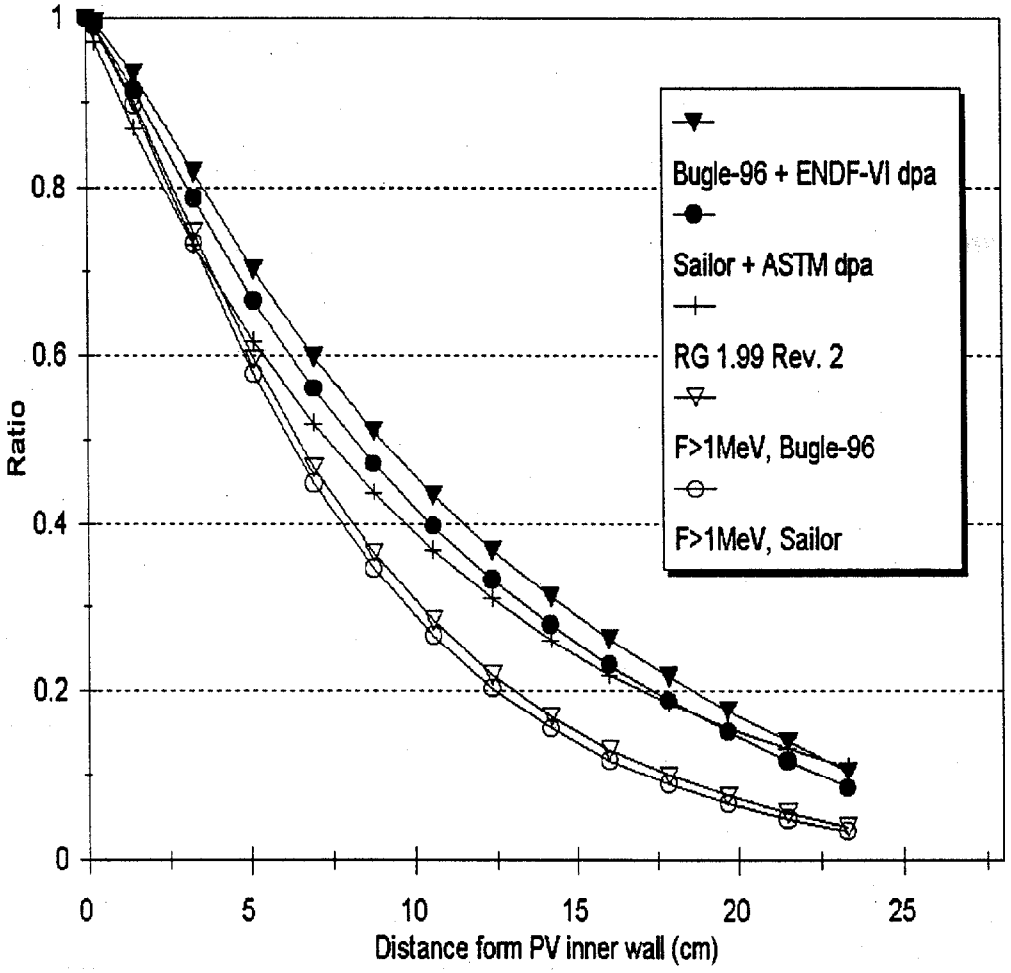

Figure 6. Flux and dpa rate attenuation in the PV wall

The extrapolation factor is defined as the ratio of the dpa rate at a given distance from the PV inner (wetted) surface to the dpa rate at the inner surface. The extrapolation factor obtained from Bugle-96 calculation with ENDF/B-VI dpa cross sections is higher than the RG 1.99 formula prediction by ~14% at ~5 cm in the PV wall and 20% at ~15 cm in the PV wall. The investigation into the causes of these large differences indicated that the RG 1.99 formula agrees within ~5% with the dpa attenuation calculated with the Sailor cross-section library, a P_1 approximation, and ASTM dpa cross sections, with the RG 1.99 still predicting faster attenuation. The difference in the dpa rate attenuation obtained with "Sailor, P_1, ASTM dpa" and "Bugle-96, P_3, ENDF/B-VI dpa" is analyzed in Table 3. Approximately 40–45% of the difference is caused by the change in cross sections (from Sailor, P_1 to Bugle-96, P_1), ~35–40% of the difference is due to the change from a P_1 to P_3 approximation to the angular dependence of the scattering cross sections, and ~15-20% of the difference is due to the change from the ASTM to the ENDF/B-VI dpa cross sections. Near the PV surfaces the calculated attenuation of the dpa rate also deviates from the simple exponential attenuation used in the RG 1.99, Rev. 2, formula, which also contributes to the differences.

Table 3. Summary of the changes in dpa attenuation at ~5 cm and 15 cm from the PV inner surface, for a 24.20-cm-thick PV wall

	Change in dpa extrapolation factor dpa(d)/dpa(d = 0) due to change from				Difference in the dpa extrapolation factor calculated with Bugle-96, P_3, ENDF/B-VI dpa cross sections and RG 1.99, Rev. 2, extrapolation formula
d*	Cross-section library from Sailor, P_1 to Bugle-96, P_1	Bugle-96, from P_1 to P_3	dpa cross sections from ASTM (ENDF/B-IV) to ENDF/B-VI	Total change	
cm	%	%	%	%	%
~5	4.2	3.7	1.6	9.8	13.8
~15	8.9	6.6	3.8	19.7	19.5

* d = distance from PV inner (wetted) surface.

CONCLUSIONS

The Bugle-96 library gives higher calculated fast neutron fluxes than the Sailor library by ~6% in the surveillance capsule and at the PV inner wall, 10% at 1/4 of the PV wall thickness, and 25% in the reactor cavity. The calculated spectra show that Bugle-96 gives group fluxes higher than the Sailor results by ~5-10% in the capsule and 20-40% in the cavity, for most of the energy groups above 0.1 MeV. The differences in the fission spectra between the Bugle-96 and the Sailor libraries have only small impacts on the calculated fast flux but are important for the comparison of the calculations and the measurements. The Bugle-96 spectra were found to give more consistent C/M ratios. The new ENDF/B-VI-based iron dpa cross sections differ considerably from the ASTM iron dpa data. However, the dpa rates (integral over energy) obtained with the two dpa cross sections agree within

~4% for the spectra throughout the PV wall. The new "Bugle-96, P_3, ENDF/B-VI dpa" calculation predicts significantly slower dpa rate attenuation through the PV wall than the old "Sailor, P_1, ASTM dpa" calculation, which is in reasonable (~5%) agreement with the RG 1.99 extrapolation formula. The differences in the flux extrapolation factors from the PV inner surface to the location at ~5 cm and 10 cm inside the PV wall (for the wall thickness of 24cm) were ~10 and 20%, respectively.

ACKNOWLEDGMENTS

This research was performed at the Oak Ridge National Laboratory, managed by Lockheed Martin Energy Research Corporation under contract DE-AC05-96OR22464 with the U.S. Department of Energy.

REFERENCES

1. R. W. Roussin, *BUGLE-80: Coupled 47 Neutron, 20 Gamma-Ray, P3, Cross-Section Library for LWR Shielding Calculations*, Informal Notes, Radiation Shielding Information Center (RSICC) Data Library Collection, DLC-075/BUGLE-80, Oak Ridge National Laboratory, 1980.
2. G. L. Simmons et al., *Analysis of the Browns Ferry Unit 3 Irradiation Experiments*, EPRI NP-3719 (November 1984), RSICC Data Library Collection, DLC-076/SAILOR; (Sailor, Coupled Self-Shielded, 47-Neutron, 20-Gamma-Ray, P_3, Cross-Section Library for Light-Water Reactors).
3. J. E. White et al., *BUGLE-96: Coupled 47 Neutron, 20 Gamma-Ray Group Cross Section Library Derived from ENDF/B-VI for LWR Shielding and Pressure Vessel Dosimetry Applications*, RSICC Data Library Collection, DLC-185, Oak Ridge National Laboratory, March 1996.
4. American National Standard, *Neutron and Gamma-Ray Cross Sections for Nuclear Radiation Protection Calculations for Nuclear Power Plants*, ANSI/ANS-6.1.2.-1999
5. E 693 Standard Practice for Characterizing Neutron Exposures in Iron and Low-Alloy Steels in Terms of Displacements Per Atom (DPA), E 706(ID), *Annual Book of ASTM Standards, Sect. 12: Nuclear, Solar, and Geothermal Energy*, 1998.
6. I. Remec and F. B. K. Kam, *H. B. Robinson-2 Pressure Vessel Benchmark*, NUREG/CR-6453, ORNL/TM-13240, Oak Ridge National Laboratory, 1998.
7. W. A. Rhoades et al., *TORT-DORT Two- and Three-Dimensional Discrete-Ordinates Transport, Version 2.8.14*, CCC-543, Radiation Shielding Information Center, Oak Ridge National Laboratory, 1994.
8. I. Remec, *Investigation of the Impact of ENDF/B-VI Cross Sections on the H. B. Robinson-2 Pressure-Vessel Flux Prediction*, ORNL/NRC/LTR-99/6, 1999.
9. *U.S. Nuclear Regulatory Commission Regulatory Guide 1.99, Revision 2*, "Radiation Embrittlement of Reactor Vessel Materials," May 1988.
10. I. Remec, J. E. White, "Development of the ENDF/B-VI Atom Displacement Cross Sections for Iron, " ORNL/NRC/LTR-99/4, Oak Ridge National Laboratory, 1999.
11. P. N. Randall, "Basis for Revision 2 of the U.S. Nuclear Regulatory Commission's Regulatory Guide 1.99," *Radiation Embrittlement of Nuclear Reactor Pressure Vessel Steels: An International Review (Second Volume)*, ASTM STP 909, L. E. Steele, Ed., American Society for Testing and Materials, Philadelphia, 1986, pp. 149–162.